6D Particle Simulation of Ion Cyclotron Resonance Heating in a Toroidal Plasma and Development of a New 5-1/2 D Gyrokinetic ICRH Particle Simulation Technique

G. Park[1,2)], C.S. Chang[2,3)]

1) National Fusion Research Center, Daejon, Korea
2) New York University, New York, NY 10012, USA
3) Korea Advanced Institute of Science and Technology, Daejon 305-710, Korea

e-mail contact of main author: gypark@cims.nyu.edu

Abstract. A six dimensional test particle simulation is performed to study the ion cyclotron resonance heating physics in a realistic toroidal magnetic field and spatially inhomogeneous wave amplitude. It is found that a more general nonlinear treatment than a quasilinear operation is necessary for a more accurate evaluation of the ICRH (ion cyclotron resonance heating) rate. Using a multi-scale approximation, we introduce a new 5-1/2 dimensional physics model, which can accurately reproduce the 6 dimensional physics by a simple extension of the conventional 5D guiding center physics to include the wave-particle gyration phase nonlinearity as well as wave amplitude inhomogeneity.

1. Introduction

Cyclotron resonance heating technique is unique in that the location of the resonance layer is controlled by the frequency of the launched wave. Due to this localization ability the cyclotron resonance heating techniques are expected to be an essential tool for localized current drive, heating, and plasma control in a future magnetic fusion reactor such as ITER (International Tokamak Experimental Reactor).

Although the quasi-linear (QL) rf heating operator is widely used for magnetically confined toroidal plasmas and highly versatile and relatively easy to implement in the interpretation of the experimental results concerning the rf-plasma interactions, there has been growing concern that the widely-used quasilinear operator to describe the wave-particle interaction physics may not be well-justified for application to a magnetic confinement device. In this work, development of a new 5-1/2D particle simulation method will be reported which can dramatically improve the numerical simulation accuracy of ICRH heated ion dynamics in magnetic fusion plasmas, which may also be used to extend in the future to improve the accuracy of the wave propagation simulations in a self-consistent manner. Here, the 1/2D represents the wave-particle phase information and finite gyro-orbit effects: Together with the guiding center (GC) equation of motion, the phase information is kept in order to evaluate the phase distortion by the collisional effect and the nonlinear wave-particle interactions and gyro effects are taken into consideration through the numerical gyroaveraging technique. This method of tracking RF heating dynamics has been incorporated into the guiding center code XGC [1] as one option; the numerical results in the following sections are all obtained by running this version of XGC.

In this paper we explain the QL prediction of the RF heating rate and compare the QL results with the ion Lorentz equation simulation ones which are the most reliable although highly time-consuming. The results from the 5-1/2D approach are also presented and compared to the QL and Lorentz equation results. Some details of the 5-1/2D GC equations of motion which contains the RF-plasma interaction terms are also presented.

2. Comparison of RF Simulation Results with QL Predictions

The most conventional QL cyclotron resonance heating operator is based on Kennel-Engelmann operator [2,3] and its bounced averaged form [4-6]. Although this theory has been highly successful in explaining many RF-related phenomena in tokamak [6], some inherent simplifications underlying the theory should not be neglected and clearly understood for its sound application to an actual experimental situation. Below we enumerate its simplifying assumptions for clarity.

1. It assumes that the resonance interaction time is short enough to neglect the non-linear RF-plasma interactions. Specifically, gyration phase nonlinearity is not included.
2. The resonance layer is thin enough to ignore the wave amplitude inhomogeneity effects seen by gyrating particles as it crosses the resonance layer.
3. Coulomb collisions are weak enough not to interfere with the QL wave-particle interaction process within a resonance layer.
4. Wave-particle phase between the consecutive resonance layers is completely decorrelated by coulomb collision or nonlinear effects such that there is no superadiabatic effect in the RF heating dynamics.
5. The respective modes (toroidal and poloidal) comprising the RF wave spectrum are completely incoherent between each other, thus individual mode is contributing to RF heating independently and there is no coherence effects between different poloidal modes.
6. Usual analytic QL theories did not take into consideration the drift particle motion (finite drift orbit width and associated radial transport) in a tokamak, i.e., the particle orbit is assumed to follow the magnetic field line and there is no cross-field drift motion.

In the past, there has been much debate over the validity of these assumptions in a realistic tokamak plasma. In fact, evidence exists in the literature that the collisional phase decorrelation is not strong enough to support the conventional understanding of ICRH interaction of energetic ions [7] although the collision is very effective at phase randomization in the presence of magnetic field inhomogeneity along the particle GC orbit for most thermal particles [3,8]. Modern wave propagation codes predict that the rf wave fields generally have strong spatial inhomogeneity and its poloidal modes spectrum is significantly wide and coherent between each other. It has been observed that finite drift orbit width effect has a nonnegligible effect on the RF heating results in DIII-D tokamak [9]. Thus, it deserves some careful work to check the validity of the QL theory against the most accurate Lorentz results. Below, we mainly concentrate on the items #1, #2, and #3.

First, let us write down a well-known QL rf operator in terms of the energy W and magnetic moment μ as the following form [4,5]:

$$\{Q(f_0)\} = \sum_{l,n} \frac{1}{\tau_b} L \tau_b D_{WW} L f_0 , \tag{1}$$

where the operator L and energy diffusion coefficient D_{WW} are defined as

$$L = \frac{\partial}{\partial W} + \frac{l\Omega}{\omega B}\frac{\partial}{\partial \mu}, \quad D_{WW} = \frac{q^2}{4\tau_b}\left| \int_0^{\tau_b} V_\perp \left[E_+ J_{l-1}\left(\frac{k_\perp V_\perp}{\Omega}\right) + E_- J_{l+1}\left(\frac{k_\perp V_\perp}{\Omega}\right)\right] e^{i\theta(t)} dt \right|^2 , \tag{2}$$

and the bounce average operation $\{\cdot\}$ [5] is defined as the time average of the quantity within the parenthesis over the unperturbed particle trajectory; similarly the time integral in the definition of D_{WW} is done over the unperturbed particle trajectory including its drift motion across the flux surfaces. Here, τ_b indicates the time for the particles to perform one poloidal transit motions, l is the cyclotron harmonic number, n is the toroidal mode number, E_+ is the

left-hand polarized component of the injected RF electric field, E_- is the right-hand component, $k_\perp$ is the local perpendicular wave vector, ω is the wave frequency, and Ω is the local cyclotron frequency. In the above, wave-particle phase difference θ is introduced such that the most significant contribution to the integral in Eq. (2) arises around the stationary phase point $d\theta/dt = \mathbf{k}\cdot\mathbf{v}_d + l\Omega - \omega = 0$, where $\mathbf{v}_d$ represents the GC velocity.

It is straightforward to calculate the QL energy variance that occurrs across the resonance:

$$\sigma_{ql}^2 = \left\langle \left(\Delta W - \langle \Delta W \rangle\right)^2 \right\rangle_{ql} = 2\tau_b D_{WW},$$

which is evaluated by inserting numerical unperturbed trajectory in the time integral operation for the definition of D_{WW} which thus naturally incorporates the finite drift orbit width effect as well as Airy function representation [10] for two close resonance points.

Let us briefly describe the numerical procedure that is followed to obtain σ^2_N (numerical energy variance). We use an EFIT tokamak magnetic field geometry under which numerical integration of equations of motion is done. Lorentz equation of motion as well as 5-1/2D GC equations is solved for each deuterium ions using a 4th order Runge-Kutta method in the presence of left-handed circularly polarized wave whose amplitude vector takes the form of $\mathbf{E}_{1A} = E_+(\mathbf{x})\left(\mathbf{e}_1 - i\mathbf{e}_2\right)$, where $\mathbf{e}_1$ and $\mathbf{e}_2$ is parallel to $\mathbf{k}_\perp$ and $\mathbf{b}$ x $\mathbf{e}_1$, respectively and span the perpendicular plane orthogonal to the local equilibrium magnetic field direction ($\mathbf{b}=\mathbf{B}_0/B_0$). We take its major radial wave number k_R and toroidal mode number n to be -60 m^{-1} and 10, respectively with k_Z=0. For the inclusion of Coulomb collision effects, we use the well-known Monte-Carlo collision scheme devised by Boozer [11] and only pitch angle scattering part of the Coulomb collision is implemented here. We assume here that test ions are collisionally scattered from realistic background plasma, whose density is 5 x 10^{13} cm^{-3} and ion temperature is 4 keV. Simulation time step for the integration of Lorentz equation is taken to be 1/ ($256f_{rf}$), where f_{rf} is the wave frequency, while that for the 5-1/2D GC equations to be one gyroperiod at the magnetic axis. The DIII-D magnetic equilibrium we use has magnetic field intensity of 2.12 T at the magnetic axis at R=1.725 m. To obtain σ^2_N, kinetic energy change ΔW_i for the ith test particle is accumulated, from which $\langle \Delta W^2 \rangle$ and $\langle \Delta W \rangle$ are obtained through ensemble averaging. The number of particles N that we use below for the average over the ensemble of particles is 100. The ensemble of particles is chosen for the wave-particle phase θ to be distributed uniformly over the particle initial conditions. Particles are initialized from the low field side of the midplane with definite values of energy and pitch and followed until they reach the high or low field side of the midplane again.

In Figs. 1 and 2 we present spatial unperturbed particle trajectories (both GC and gyro-orbits) projected on the poloidal cross section (Fig. 1) and the temporal evolution of the energy variances (Fig. 2) for 40keV trapped particles under the RF field with constant amplitude (E_+ ($\mathbf{x}$) =E_{+0} =6kV/m) for l=1. The trapped particle's initial pitch value is appropriately set ($v_{||}/v$ = 0.475) for the banana turning point to be formed inside the cyclotron resonance layer. The downward arrow in Fig. 2 indicates the time instant after which pitch angle collisions are turned on. From Fig. 2, it can be clearly seen that the RF heating rate, i.e., energy variances, are greatly overestimated by the QL prescription in the trapped particle case. The reason for this great overestimation of the QL theory in predicting the energy variances may be attributed to the fact that actual resonant particle orbits can not be approximated well by the unperturbed ones in the calculation of RF diffusion coefficients (Eq. (2)) when RF heating geometry imposes the long duration of particle orbit within the resonance region as in Fig. 1,

thus violating QL assumption #1. Note that this case corresponds to the vanishing second derivative of θ at the resonance, i.e., $\ddot{\theta}_{res} \to 0$ and usually has been treated by using an Airy function representation without due consideration of the nonlinear effects.

In Figs. 3 and 4, energy increments $\delta W=\Delta W-\langle\Delta W\rangle$ vs. initial wave-particle phase θ_0 (Fig. 3) and the energy variance σ^2 versus E field strength E_{+0} (Fig. 4) are shown for the same parameter values as in Figs. 1 and 2. Fig. 3 clearly shows the typical sinusoidal variation of δW with the wave-particle phase θ_0 for the QL results while the actual Lorentz simulation results show a rather nontrivial behavior as a function of θ_0. Notice that 5-1/2D model accurately gives the same results as those from the Lorentz simulations. As for the effects of collisions we can see that its main effect is to bring about some random fluctuations of δW around the collisionless values, whereas statistically averaged quantities such as the energy variance are little affected by the collision as can be seen in Fig. 4. Therefore, assumption #3 can be said to be valid generally in an averaged sense. As expected easily, the deviation of QL results from the Lorentz ones gets larger as the E field strength increases because the larger the E field strength is, the more the nonlinear orbit perturbation results.

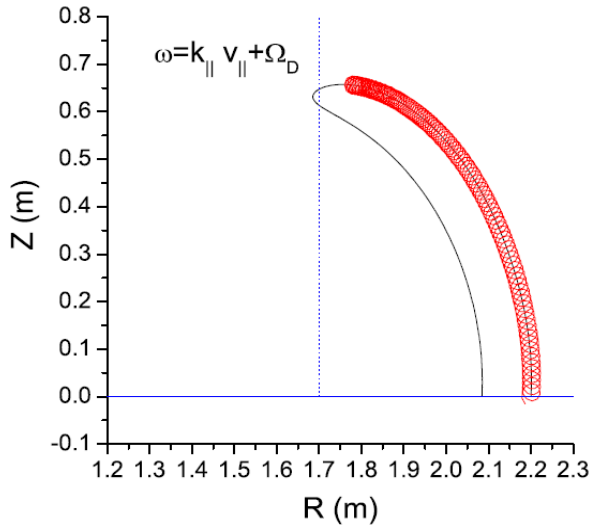

FIG. 1. Guiding and gyro orbits on poloidal plane.

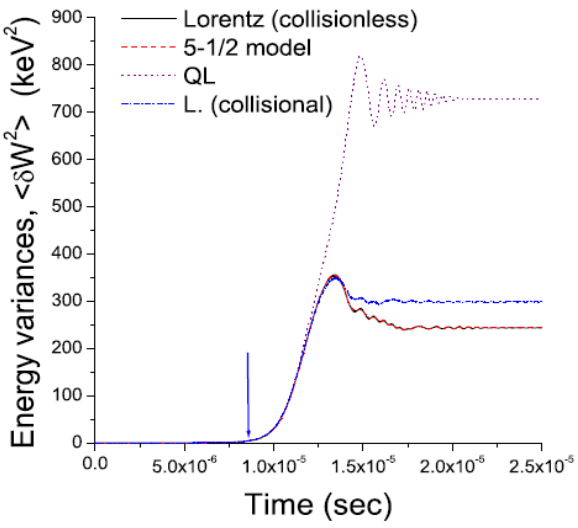

FIG. 2. σ^2 versus time.

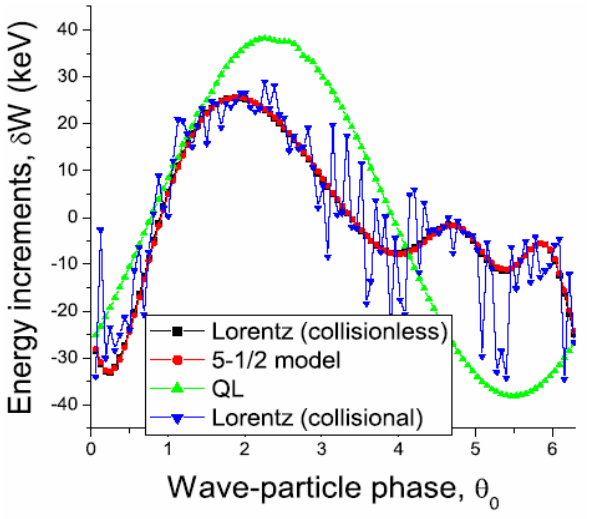

FIG. 3. δW versus θ_0 for E_{+0} =6kV/m.

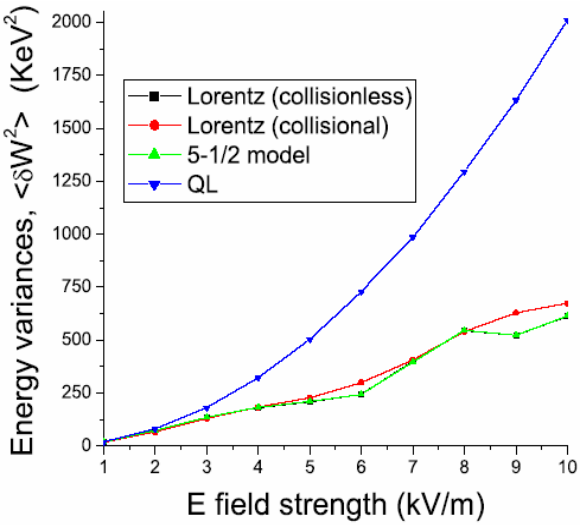

FIG. 4. σ^2 versus E_{+0}.

Fig. 5 shows the energy variance σ^2 versus E field strength E_{+0} . Initial pitch value is set to 0.8 and the other parameters are the same as in Figs. 1–4 . Contrary to the trapped particle cases we can that there is a good agreement between the QL and Lorentz simulation results, which implies that passing particle heating dynamics can be well described by the QL theory.

Finally, Fig. 6 represents the effects of the wave amplitude inhomogeneity E_+ (**x**) on the RF heating results. Here, we model a RF amplitude gradient near the cyclotron resonance layer in a tokamak geometry as a tangent hyperbolic form represented as

$$E_+(R,Z) = E_{+0}\left[1+\tanh\left((R-R_{inhom})/L_R\right)\right],$$

where R_{inhom} is the major radius of the center of amplitude variation and L_R is the width of the strong amplitude gradient region. We take the values of R_{inhom} and L_R to be 1.7m and 2.5 cm, respectively; note that the value of L_R is comparable to the gyroradius size at the resonance (≈ 3cm) of the 100 keV deuterium ions. RF-induced energy variances versus E_{+0} are plotted in Fig. 6 for the case of 100 keV trapped particles ($v_{||}/v$ = 0.475) for fundamental harmonic case with the heating geometry as in Fig. 1. We can see that the RF-induced energy variances are much enhanced in magnitude by the wave amplitude inhomogeneity effects compared to the QL results. Again, 5-1/2D model gives the correct description of Lorentz simulation results. The failure of the QL theory in this case can be understood by considering that the resonance region may be sufficiently wide enough for the gyrating particles to feel the detailed spatial amplitude variation along their gyro-orbits. Therefore, the QL assumption #2 can be violated as well for the strongly inhomogeneous spatial wave structure and large gyro-orbit particles. The usual Bessel function in the QL diffusion coefficient in Eq. (2) should, then, be replaced by the more general expression incorporating actual spatial wave variation.

The main intention of the simulation results in this section is to reveal the possible erroneous predictions of the QL theory and how it can be cured by the 5-1/2D GC model which is constructed to overcome the incapability of QL theory. In the next section, we will discuss some details of the 5-1/2D GC approach.

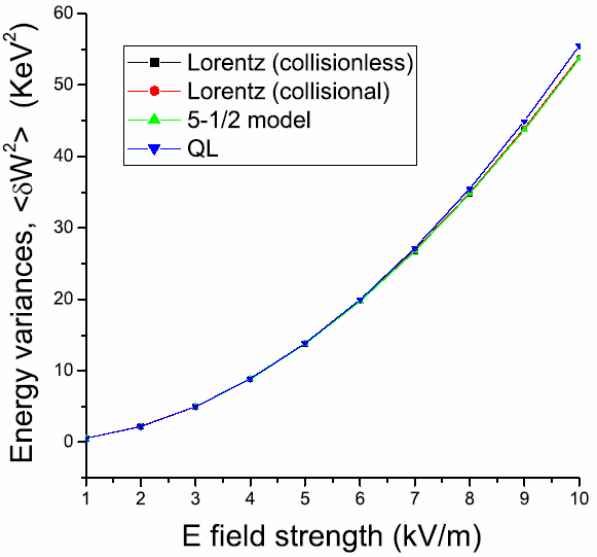

FIG. 5. σ^2 versus E_{+0} for passing particles with constant E_+ profile.

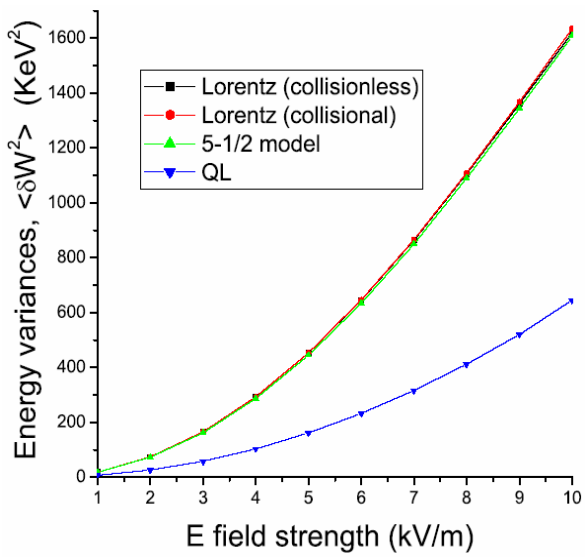

*FIG. 6. σ^2 versus E_{+0} for nonuniform E_+ (**x**)*

3. Guiding-Center Motion in the Presence of High Frequency RF Wave with Cyclotron Resonance

Let us first start from the Lagrangian represented in terms of Littlejohn's standard GC variables $\mathbf{Z}=(\mathbf{X}, \rho_{||}, \mu, \phi)$ [12,13] as

$$\Gamma = \frac{q}{c}\mathbf{A}^*\left(\mathbf{X},\rho_{\|},\mu\right)\cdot d\mathbf{X} + \frac{B_0}{\Omega}\mu d\phi - H_0 dt + \frac{q}{c}\mathbf{A}_1\left(\mathbf{X}+\boldsymbol{\rho},t\right)\cdot d(\mathbf{X}+\boldsymbol{\rho}) = \Gamma_0 + \Gamma_1, \qquad (3)$$

where $\mathbf{X}$ represents the GC position, $\rho_{||} = v_{||}/\Omega$ normalized parallel velocity, $\mu = m v_{\perp}^2/2B_0$ ($\mathbf{X}$) the magnetic moment, ϕ gyrophase, $\boldsymbol{\rho}$ gyroradius vector, $\mathbf{A}_1$ vector potential of the RF perturbation part, H_0 unperturbed Hamiltonian, Γ_0 unperturbed Lagrangian, and Γ_1 perturbed Lagrangian. The guiding center variables are a special set of coordinates in which the gyromotion is decoupled from the main GC dynamics in the absence of the wave perturbation. In Eq. (3), H_0, and $\mathbf{A}^*$ are defined by

$$H_0\left(\mathbf{X},\rho_{\|},\mu\right) = \frac{q^2}{2mc^2}B_0^2(\mathbf{X})\rho_{\|}^2 + \mu B_0(\mathbf{X}),$$

$$\mathbf{A}^*\left(\mathbf{X},\rho_{\|},\mu\right) = \mathbf{A}_0(\mathbf{X}) + \rho_{\|}\mathbf{B}_0(\mathbf{X}) - \frac{mc^2}{q^2}\mu\mathbf{W}(\mathbf{X}), \quad \mathbf{W}(\mathbf{X}) = (\nabla\mathbf{e}_1)\cdot\mathbf{e}_2 + \frac{\mathbf{b}}{2}(\mathbf{b}\cdot\nabla\times\mathbf{b}).$$

Due to the presence of the wave perturbation $\mathbf{A}_1$, the Lagrangian Γ depends on the fast gyromotion time-scale dynamics through Γ_1 which should also be averaged.

In order to remove the fast time-scale dynamics brought about by the perturbation Γ_1 from the main averaged GC equations of motion which we are seeking for, we can follow the Lagrangian Lie coordinate transformation perturbation method [14-16] which gives the new averaged coordinates $\bar{\mathbf{Z}} = \left(\bar{\mathbf{X}}, \bar{\rho}_{||}, \bar{\mu}, \bar{\theta}\right)$ and Lagrangian $\bar{\Gamma}$ in the form of

$$\bar{\Gamma} = \frac{q}{c}\left[\mathbf{A}^*\left(\bar{\boldsymbol{X}},\bar{\rho}_{\|},\bar{\mu}\right) - \frac{c\bar{\mu}B_0}{ql\Omega}\mathbf{k}\right]\cdot d\bar{\mathbf{X}} + \frac{B_0}{l\Omega}\bar{\mu}d\bar{\theta} - \left(\bar{H}_0 - \frac{B_0}{l\Omega}\bar{\mu}\omega + \bar{H}_1\right)dt, \qquad (4)$$

where we use the wave-particle phase difference $\bar{\theta}$ as one phase space variable instead of $\bar{\phi}$ because it is slowly varying near the lth harmonic cyclotron resonance surfaces, thus suitable for the averaged variable. Note that in the present case of resonant interaction with high wave frequency on the order of gyrofrequency, gyrophase dynamics is not completely decoupled from the main GC dynamics. Comparing Eqs. (3) and (4) it can be seen that the wave term perturbing the symplectic structure of the Lagrangian Γ is thrown into the Hamiltonian component ($\bar{H}_1$) for the new $\bar{\Gamma}$, which can be realized through careful determination of the generating vector $\mathbf{G}_1$ and gauge function S_1 in the Lie transformation methodology[14-16]. The explicit form of the first-order perturbed Hamiltonian $\bar{H}_1$ is

$$\bar{H}_1\left(\bar{\mathbf{X}},\bar{\rho}_{\|},\bar{\mu},\bar{\theta}\right) = -\overline{\Gamma_{1i}\left(\frac{d}{dt}\right)_0\bar{Z}^i} = \frac{iq}{\omega}\left\langle\mathbf{v}(\bar{\mathbf{Z}})\cdot\mathbf{E}_1(\bar{\mathbf{X}}+\bar{\boldsymbol{\rho}},t)\right\rangle_l = \bar{H}_{1A}\left(\bar{\mathbf{X}},\bar{\rho}_{\|},\bar{\mu}\right)e^{i\bar{\theta}}, \qquad (5)$$

where $(d/dt)_0$ is the time rate of change of the operand evaluated along the unperturbed GC orbit given by Γ_0, the overline symbol above $\overline{\Gamma_{1i}\left(d/dt\right)_0\bar{Z}^i}$ stands for extracting slowly varying part of that or averaging over gyroperiod time scale, the angular braket notation with subscript l denotes the lth gyroharmonic component, and $\mathbf{v}(\bar{\mathbf{Z}})$ is a velocity vector (neglecting drift component) represented in terms of $\bar{\mathbf{Z}}$.

Applying the Euler-Lagrange equations to the Lagrangian $\bar{\Gamma}$, 5-1/2D averaged GC equations of motion with RF interaction terms can be obtained as follows:

$$\frac{d\bar{\mathbf{X}}}{dt} = \frac{1}{B_{\|}^{*}}\left[\left(\Omega\bar{\rho}_{\|}+\frac{1}{m\Omega}\frac{\partial\bar{H}_{1A}}{\partial\bar{\rho}_{\|}}e^{i\bar{\theta}}\right)\mathbf{B}^{*}+\frac{c}{q}\mathbf{b}\times\left(\nabla\bar{H}_{0}+(\nabla\bar{H}_{1A}+i(\mathbf{k}+l\mathbf{W})\bar{H}_{1A})e^{i\bar{\theta}}\right)\right], \quad (6)$$

$$\frac{d\bar{\rho}_{\|}}{dt} = -\frac{\mathbf{B}^{*}}{m\Omega B_{\|}^{*}}\cdot\left[\nabla\bar{H}_{0}+(\nabla\bar{H}_{1A}+i(\mathbf{k}+l\mathbf{W})\bar{H}_{1A})e^{i\bar{\theta}}\right], \quad (7)$$

$$\frac{d\bar{\mu}}{dt} = -\frac{il\Omega}{B}\bar{H}_{1A}e^{i\bar{\theta}}, \quad (8)$$

$$\frac{d\bar{\theta}}{dt} = (\mathbf{k}+l\mathbf{W})\cdot\frac{d\bar{\mathbf{X}}}{dt}+l\Omega-\omega+\frac{l\Omega}{B}\frac{\partial\bar{H}_{1A}}{\partial\bar{\mu}}e^{i\bar{\theta}}, \quad (9)$$

where $\mathbf{B}^{*}=\nabla\times\mathbf{A}^{*}$ and the three finite Larmor radius functions $\bar{H}_{1A}$, $\nabla\bar{H}_{1A}$, $\partial\bar{H}_{1A}/\partial\bar{\mu}$ are defined for an arbitrary spatial wave structure as

$$\bar{H}_{1A} = \frac{iq}{\omega}\sqrt{\frac{2\bar{\mu}B_{0}(\bar{\mathbf{X}})}{m}}\int_{0}^{2\pi}\frac{d\bar{\phi}}{2\pi}E_{+}\left(\bar{\mathbf{X}}+\bar{\boldsymbol{\rho}}\right)e^{i\mathbf{k}\cdot\bar{\boldsymbol{\rho}}-i(l-1)\bar{\phi}}, \quad (10)$$

$$\nabla\bar{H}_{1A} = \frac{\nabla B_{0}}{2B_{0}}\bar{H}_{1A}+\frac{iq}{\omega}\sqrt{\frac{2\bar{\mu}B_{0}(\bar{\mathbf{X}})}{m}}\int_{0}^{2\pi}\frac{d\bar{\phi}}{2\pi}\left\{\nabla E_{+}\left(\bar{\mathbf{X}}+\bar{\boldsymbol{\rho}}\right)+i\nabla(\mathbf{k}\cdot\bar{\boldsymbol{\rho}})E_{+}\right\}e^{i\mathbf{k}\cdot\bar{\boldsymbol{\rho}}-i(l-1)\bar{\phi}}, \quad (11)$$

$$\frac{\partial\bar{H}_{1A}}{\partial\bar{\mu}} = \frac{1}{2\bar{\mu}}\bar{H}_{1A}+\frac{iq}{\omega}\sqrt{\frac{2\bar{\mu}B_{0}(\bar{\mathbf{X}})}{m}}\int_{0}^{2\pi}\frac{d\bar{\phi}}{2\pi}\frac{\partial\bar{\boldsymbol{\rho}}}{\partial\bar{\mu}}\cdot\left\{\nabla E_{+}\left(\bar{\mathbf{X}}+\bar{\boldsymbol{\rho}}\right)+i\mathbf{k}E_{+}\right\}e^{i\mathbf{k}\cdot\bar{\boldsymbol{\rho}}-i(l-1)\bar{\phi}}, \quad (12)$$

which can be numerically calculated as a discrete sum over N_g gyropoints. As for the magnitude of N_g we used ten points approximation although it can be varied depending on the characteristics of the wave perturbation and particle energy. Let us point out the main improvements of the above 5-1/2D GC equations over the QL method:

1. The 5-1/2D equations are nonlinear in the GC variables and thereby can account for the nonlinear RF-plasma interaction process.
2. Arbitrary spatial wave structures, such as broad poloidal modes spectrum and highly inhomogeneous amplitude profiles, can be retained in the calculation through the numerical gyroaveraging technique applied to Eqs. (10) –(12).
3. Phase correlations between distinct resonance interactions and associated superadiabatic effects are also covered under the 5-1/2D equations because phase information is kept along the repeated particle transit motions over the poloidal direction.
4. Finite particle drift orbit width and associated radial transport effects are naturally built into the model.

Therefore, it is obvious that the 5-1/2D GC model can correct almost all deficiencies, i.e., simplified assumptions that we have mentioned in Sec. 2, of the current QL theory about tokamak RF-plasma interaction phenomena. Although Eqs. (10) –(12) contain only the left-hand component E_{+}, it can be straightforwardly extended to include the right-hand component E_{-} as well.

4. Conclusion and Discussions

In this work, the validity of the various QL assumptions has been checked numerically against the 6D particle simulation results using a realistic DIII-D magnetic equilibrium (g-eqdsk file). The importance of the nonlinear wave-particle interaction for a tokamak plasma ions, the significance of the wave-field inhomogeneity, and the collisional effects on the heating rate has been demonstrated. To incorporate these nonconventional effects, we introduce a 5-1/2D GC equation approach which can accurately account for the nonlinear as well as wave-field inhomogeneity effects in a GC time scale without the need to resolve detailed ion gyration dynamics. The 5-1/2D simulation results has been verified against the 6D simulation results.

For the substantial speed up of the numerical GC simulation with 5-1/2D model it may be preferred that the RF-dependent parts of the GC equations are only turned on in the vicinity of cyclotron resonance surfaces; outside which normal unperturbed GC orbits can be followed. Moreover, for most passing orbits except for those tangent to the resonance surface for off-magnetic axis heating situation the conventional QL heating scheme can be applied in good accuracy, which can additionally reduce the simulation time cost. Therefore, it is certain that there are various efficient ways of combining 5-1/2D and conventional QL schemes.

In the literature high-frequency gyrokinetic formalism [17,18] has been developed which, in most cases, was linearized and thereby losing the possibly important nonlinear effects on RF heating dynamics. Our construction of 5-1/2D equations tries to avoid this simplification and retain important effects of nonlinear wave-particle interaction and detailed spatial wave structure which could cause a large difference of actual heating rate from the conventional QL results as we have seen in this paper.

Acknowledgement
This work was supported by the Korean KSTAR Project and US DOE.

References

[1] CHANG, C. S., KU, S., and WEITZNER, H., Phys. Plasmas **11** (2004) 2649.
[2] KENNEL, C. F., and ENGELMANN, F., Phys. Fluids **9** (1965) 2377.
[3] STIX, T. H., Nucl. Fusion **15** (1975) 737.
[4] HAMMET, G. W., Fast Ion Studies of Ion Cyclotron Heating in the PLT Tokamak, Ph.D. thesis, Princeton University, Plasma Physics Laboratory (1986).
[5] CHANG, C. S., LEE, J. Y., and WEITZNER, H., Phys. Fluids B **3** (1991) 3429.
[6] STIX, T. H., Waves in Plasmas, American Institute of Physics, New York (1992).
[7] BERGEAUD, V., et al., Phys. Plasmas **8** (2001) 139.
[8] KASILOV, S. V., et al., Nucl. Fusion **30** (1990) 2467.
[9] CHOI, M., et al., Phys. Plasmas **12** (2005) 072505.
[10] KERBEL, G. D. and MCCOY, M. G., Phys. Fluids **29** (1985) 3629.
[11] BOOZER, A.H., KUO-PETRAVIC, G., Phys. Fluids **24** (1981) 851.
[12] LITTLEJOHN, R. G., J. Plasma Phys. **29** (1983) 111.
[13] BRIZARD, A. J., J. Plasma Phys. **41** (1989) 541.
[14] LITTLEJOHN, R. G., J. Math. Phys. **23** (1982) 742.
[15] CARY, J. R. and LITTLEJOHN, R. G., Ann. Phys. **151** (1983) 1.
[16] Ye, H. and KAUFMAN, A. N., Phys. Fluids B **4** (1992) 1735.
[17] CHEN, L. and TSAI, S. T., Plasma Phys. **25** (1983) 349.
[18] Chiu, S. C., et al., Phys. Plasmas **7** (2000) 4609.